Use of nano-magnetic materials for removal of lead (II) and cadmium (ii) ions from aqueous solutions

A.Y. Hammood[1*], T.E. Jassim[2] and M.J.K. Al-Asadi[2]
*[1]Marine Science Center, [2]College of Education for Pure Science,
University of Basrah, Iraq
e-mail: ahmed_yh79@yahoo.com

Abstract - Ferrite nanoparticles (NPs) with structure $NiFe_2O_4$ were created following the sol-gel auto-combustion method using lemon juice as surfactant and fuel agent. This method is located within the green chemistry, a method of environmentally friendly and less expensive than other methods. Nanomaterial's have been diagnosed using different physical and chemical techniques: Brunauer-Emmett-Teller (BET) analysis, Field Emission-Scanning Electron Microscopy (FE-SEM), Energy Dispersive X-ray Spectroscopy (EDX), Fourier-Transform Infrared Spectroscopy (FTIR), Transmission Electron Microscopy (TEM) and X-ray diffraction (XRD). X-ray diffraction patterns confirmed the phase purity and the particle size 24.27nm. The effects of adsorbent concentration, pH, temperature, and time of contact on Lead and Cadmium ions uptake behavior were measured. The optimum time of contact to attain equilibrium is 60min for Lead (II) ion and 90 min for Cadmium (II) ion, and pH values are in the range (3-9). The results of adsorption showed a strong correlation with Freundlich model compared with the Langmuir model. The thermodynamic parameters were given, revealing endothermic reaction for ΔH, ΔG was found a spontaneous process and ΔS had positive value, increase of disorder of the process.

Introduction

After fast growth of population and manufacture societies, the release of heavy metals into the environmental water system is one of the most important environmental concerns. Despite that most of the harmful chemical materials when they are in the atmosphere after some years become less dangerous. When pollution by heavy metal ions occurred, removing them are extremely difficult and maybe gradually built up and enter to our body across food chains (Khoshkerdar and Esmaeili, 2019; Luo *et al.*, 2015). Heavy metals are one of the most important pollutants among the different types of water pollutants. They are characterized by severe toxicity even at very low concentrations and are stable in the environment, threatening living organisms and the environment in general. (Seiler *et al.*, 1988; Yadanaparthi *et al.*, 2009). There are several sources of pollution of the water environment with heavy elements, of which electronic industries, electroplating industry, coal-fired electric power stations, tanneries and other industries (Wang and Chen, 2009; Yin *et al.*, 2010).

Water pollution is one of the modern issues by dangerous metal particles like Cd(II), Pb(II) and contamination by microorganisms that causes the saturation of danger in the water and turn into a serious natural medical problem and a general seriousness.

A lot of materials are used to remove heavy metals particularly if they are able to remove the ions but relies on which is your interest in the activity and performance of the process. So many ways were established to guide the waste, such as water precipitation, Commerce Particles, float, Electrochemical oxidation drugs, adsorption, invert osmosis, dissipation, film filtration, and biosorption procedures are widely used (Chen *et al.,* 2009; Ivanov *et al.,* 2004).

The adsorption method has been recognized as a very efficient and economical method (Chai *et al.*, 2013). Since the adsorption mainly depends on the properties of the adsorbent, the selection of a suitable adsorbent is essential. There is currently much research focused on adsorbents for cadmium removal (Chen *et al.*, 2011), inclusively zeolite, activated carbon Red clay, chitosan, resins and Red clay (Liu *et al.*, 2018). However, these materials have some minor disadvantages in their applications, such as poor adsorption capacity, poor adsorption efficiency, or separation problems. In the last few years, there was an increased interest in spinel ferrites having a new row of being favorites for the purpose of water treatment (Masunga *et al.*, 2019; Kefeni *et al.*, 2017). This material has a high surface area as well as contains active places for interacting with the pollutants, thus saving a high absorption capability. Spinel ferrites have possessions super paramagnetic properties (SPM), enabling them to be quickly retrieved From the reaction combination with the use of an external magnetic field (Baig and Varma, 2013; Baig *et al.*, 2015). Spinel ferrites have been studied for their ability to remove organic compounds, nutrient salts, and toxic metals from water (Tran *et al.*, 2020).

The general chemical formula for magnetic spinel ferrites nanoparticleMFe_2O_4 (where $M = Co^{2+}$, Ni^{2+}, Mn^{2+}, Zn^{2+} . . .) provides great magnetic adjustability by changing its size and chemical composition as the high surface area enhances its ability to remove elements (Wang *et al.*, 2004; Yavuz *et al.*, 2006).

These compounds are prepared as powders or thin films by different methods and techniques. The sol-gel technique is considered as the most common methods (Prasad and Gajbhiye, 1998; Dehghanpour, 2016), ball milling technique (Abdel-Latif, 2012), precipitation (Shi *et al.*, 1999), Electrode spinning method (Tan *et al.*, 2009; Nejati and Zabihi, 2012), Hydrothermal method (Salavati *et al.*, 2009), the process of reverse micelles (Maaz *et al.*, 2009), Exact emulsion method (Kavas *et al.*, 2009) and the auto-combustion sol-gel method (Ismat *et al.*, 2017). In the current work, $NiFe_2O_4$ the ferrite sample was prepared on the basis of the method of sol-el auto-combustion employ Lemonade as a surfactant and a fuel agent. The effect of lemon juice on nitrates, works in the way that lemon juice attachs the metal ions under the assumption that metal ions substitute the hydrogen from –COOH groups in the lemon juice.

When the citric acid molecules in lemon juice as chelating agent could orient in different directions, hence, the obtained particles had little opportunity for connecting together (Gholipour and Rahimi-Nasrabadi, 2019). This technology is considered environmentally friendly and cost effective against the conventional synthesis of technologies. This labor relates to one of the applications from the adsorption behavior of an aqueous solution. The susceptibility of the produced nanomaterials as adsorbents of Lead and Cadmium ions was examined on the surface of the prepared nanomaterial. The objective of this work is to find for a surface that is with a high degree of Portability for pb(II) and Cd(II) ions adsorption, be used in the process of contamination of the aqueous solution in nature.

Materials and Methods

Synthesis of $NiFe_2O_4$ nanoparticles:

The process for synthesis of $NiFe_2O_4$ was carried out as in the following:

1. 14.54g of $Fe(NO_3)_3.9H_2O$ (M.W 404) was mixed with 5.26g of $Ni(NO_3)_2.6H_2O$ (M.W 290.69) and dissolved in 45ml of lemon juice extract.
2. Ammonia solution (NH_4OH) was added in order to keep the pH of the solution at 7.0 with continuous stirring using a magnetic stirrer.
3. Continuous stirring for 30min at 80°C, the clear sol. was completely turned to a gel.
4. Oven desiccate at 80°C to get a steady weighing and grinded to fine powder, then calcined at 600°C for 5 hours in furnace under air atmosphere.

Characterization techniques:

For the purpose of diagnosis, many advanced and highly efficient technologies that are used worldwide have been used. These are represented by X-ray diffraction (XRD), transmission electron microscopy (TEM), Brunauer-Emmett-Teller (BET) to find out the surface area, scanning electron microscopy with energy dispersive X-ray spectroscopy (FESEM-EDX). For calculation of the Pb(II) the flame atomic absorption spectrophotometer (AAS) has been used.

Adsorption Studies:

The stock solution of Lead and Cadmium have been made by melting 1.59g of lead nitrate $Pb(NO_3)_2$ and 2.74g of $Cd(NO_3)_2.4H_2O$ in 1000ml of deionized water, from this concentration several other dilute solutions were prepared. To determine the ideal pH, both HCl (0.1M) and NaOH (0.1M) were used to keep the pH range at 3-9. Perfect contact time 5-180min for adsorption of Pb(II) and Cd(II) ions was determined using batch method, where 0.05g of the absorbent has been added to a 25ml solution with concentration of 100 $mg.l^{-1}$ of Pb(II) and 20 $mg.l^{-1}$ of Cd(II) placed in 100ml flasks. Different temperature is 10.0, 25.0, 37.5 and 50.0°C, were used for equilibration, with agitation rate of 120 rpm using an orbital shaker. The amount of ions adsorbed and removal percent of adsorbent depending on the difference between concentration of the ion before and after adsorption were obtained from equations (1) and (2) (Jain *et al.*, 2019).

$Qe = V(C_o – C_e)/m$ ....(1)

removal % = $[(C_o – C_e)/C_o] \times 100$.........(2)

Where; Q_e is the maximum capacity of adsorption at equilibrium (mg/g), V is the volume of solution (l), m is the weight of the adsorbent material (g), C_o is the first concentration of the solution in $mg.l^{-1}$, C_e is the concentration of the solution in $mg.l^{-1}$ after adsorption. Langmuir and Freundlich isotherms were used to analyze the adsorption data.

Thermodynamic Parameters:

From the stock solution of Pb(II) different concentrations with ranges of 60-120$mg.l^{-1}$ and the 5-30$mg.l^{-1}$ of Cd(II) have been prepared, placed in flasks and subsequently 0.05g $NiFe_2O_4$ was added to every concentration. The flasks were shaked at 120rpm and in the right balance time at different temperatures 10.0, 25.0, 37.5 and 50.0°C. The mixture was centrifuged and the lead ion concentration was determined. ΔG is the variations in free energy, enthalpy ΔH and entropy ΔS related to the adsorption process were calculated using equations (3-5).

ΔG = -RT lnk......................(3)

K = C_{solid} / C_{liquid}.................(4)

lnK = ΔS / R – ΔH / RT......(5)

Where ΔG is the Gibbs free energy (KJ.mol^{-1}), K is the equilibrium constant, C_{solid} is the concentration of solid phase at equilibrium (mg/l), C_{liquid} is the concentration of liquid phase at equilibrium (mg/l), T is the temperature in Kelvin and R is the constant gases (0.0083 KJ.K^{-1}.mol^{-1}). ΔH (KJ.mol^{-1}) and ΔS (KJ.mol^{-1}.K^{-1}) were calculated by the values of the slope and the intersection using the equation.(5) (Ge and Ma, 2015).

Results and Discussion

FT-IR Spectroscopy:

The FTIR spectra of the sample calcified at 600°C are shown in Figure (1). The infrared spectrum recorded many absorption peaks at the range 4000cm^{-1} to 400cm^{-1}. The peak observed at 3441.01cm^{-1} may be attributed to the stretching vibration of the hydroxide(O-H) bond, which indicates the adsorption of water on ferrite (Anandan and Rajendran, 2011). The position of spinel ferrite finds in the region of 400-600cm^{-1} by (Ni-O) and (Fe-O) is stretching vibration (Kareem and Rajeh, 2018).

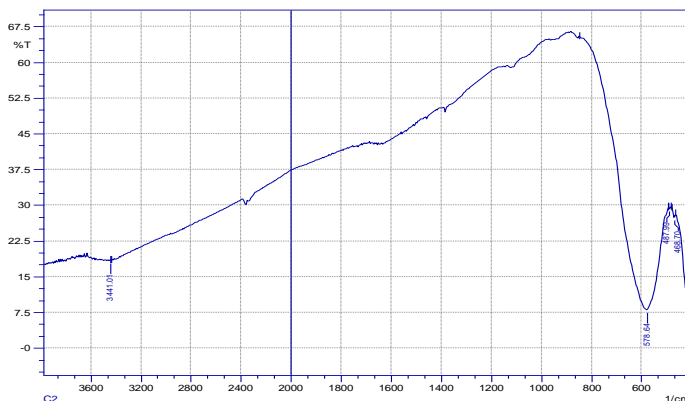Figure 1. FT-IR spectra of $NiFe_2O_4$.

X-ray Diffraction (XRD):

The results in Figure (2) showed the identification of (NiFe2O4) sample prepared by using X-ray diffraction technique. The spectrum of the prepared sample exhibited crystalline and monophasic properties. The standard data (JCPDS file No: 10-325) for $NiFe_2O_4$ (Sezgin *et al.*, 2013) has been used for comparison with the present results, and proved that both of the two study samples can be included within the spinel cubic designated in the reflecting planes (111), (220), (311), (400), (422), (511), (440) and (533) in the patterns. The size of the crystals for the X-ray spectrum and for plane (311) were calculated using the Debye-Scherrer equation:

τ_{hkl} $_=$ (K*λ)/ (β_{hkl}*cos(θ_{hkl})) .... (6)

Where τ is the particle size perpendicular to the natural line of (hkl) plane, β_{hkl} is the full width at half maximum, θ_{hkl} is the Bragg angle of (hkl) peak, K is constant equals to 0.9 and λ is the wavelength of the X-ray (Cullity, 1978). The particle size of nanoparticles calculated is about 24.27nm for $NiFe_2O_4$.
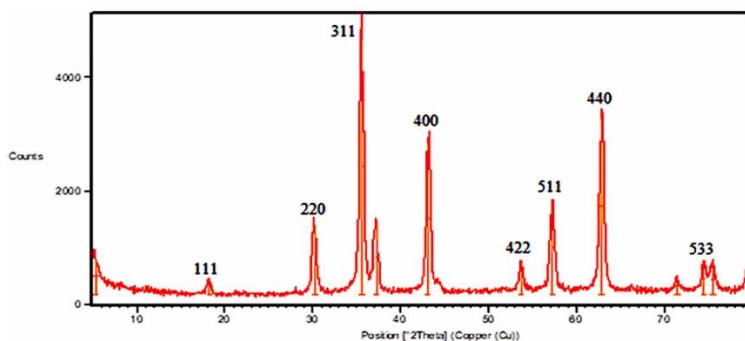
Figure 2. XRD spectrum of NiFe$_2$O$_4$.

Surface Morphology and Elemental Analysis:

  Field Emission Scanning Electron Microscopy (FESEM) was used to investigate the morphology of the as-prepared nanoparticles. Figure (3) showed that the bare NiFe$_2$O$_4$ particles were quasi-spherical with small agglomeration. On the other hand, Figure (4) represented the TEM images NiFe$_2$O$_4$ nanoparticles, the image showed the presence of pores and voids within a network formed as a result of the deposition of gases through the reaction of combustion. This finding is typical of combustion-synthesized powders.
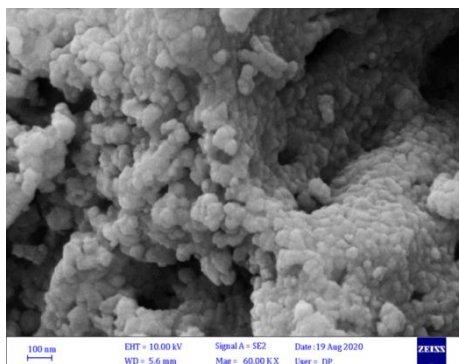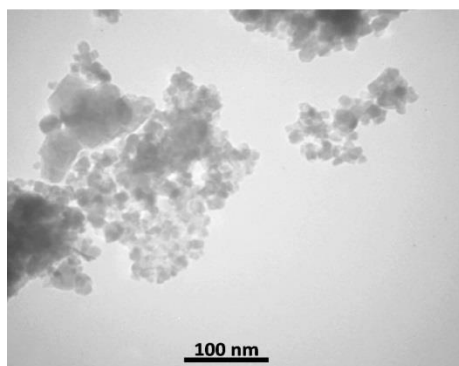

Figure 3. FESEM images of NiFe$_2$O$_4$.

Figure 4. TEM micrograph of NiFe$_2$O$_4$.

The samples of the particles are roughly spherical. Compositional purity was confirmed by analysis (EDX) of various regions of each sample. In addition the use of EDX technology offers many possibilities in terms of sample components and elements' mapping. Figure (5) and as a Table (1) showed the EDX spectrum of the prepared NiFe2O4. Through the results, it is clear that the elements Ni, O and Fe was present in different proportions the presence of impurities are very low.
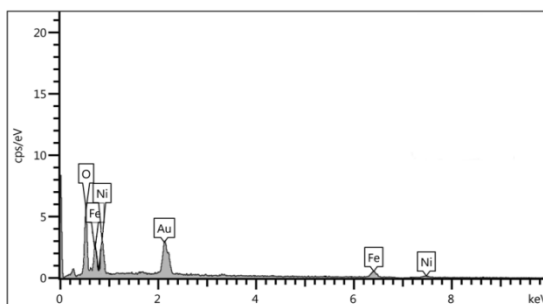

Figure 5. EDX spectra of $NiFe_2O_4$.

Table 1. Elements percentage calculated by EDX analysis.

Element	Weight %
Fe	42.8
Ni	23.4
O	33.3
Co	0.2
Zn	0.3
Total %	100

Brunauer-Emmett-Teller (BET):

The nitrogen adsorption-desorption isotherms of $NiFe_2O_4$ NPs have studied using Brunauer-Emmett-Teller (BET) analysis (Fig. 6). The BET surface area of $NiFe_2O_4$ NPs was found to be $3.91 m^2.g^{-1}$. The higher surface area of nanoparticles $NiFe_2O_4$ can be attributed to the reduced grain size. Figure (6) showed the size and distribution of pores in the prepared nanoparticles.

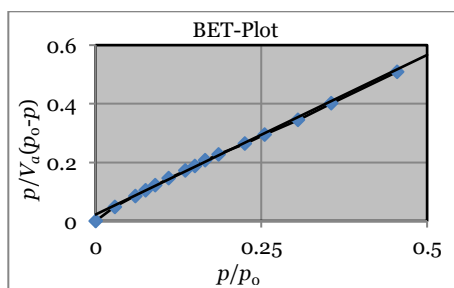Figure 6. BET of $NiFe_2O_4$.

The average pore diameter of the nanoparticles $NiFe_2O_4$ is 7.99nm (Table 2). The average pore diameters were received from ferrite due to the intra-granular pores formative into the metal oxides.

Tables 2. Specific size and surface area of the examined samples.

BET plot		C	Languer plot		B	t-plot $a(m^2.g^{-1})$	BJH plot		Peak (Area), R_p (nm)
Vm $(cm^3.g^{-1})$	a $(m^2.g^{-1})$		Vm $(cm^3.g^{-1})$	a $(m^2.g^{-1})$			Vm $(cm^3.g^{-1})$	a $(m^2.g^{-1})$	
0.90	3.91	49.97	0.90	3.94	0.89	3.22	0.06	5.38	7.99

Adsorption Studies:

Effect of Contact Time:

Different periods of time (5-180min), at fixed temperature (25°C) were used to investigate the influence of contact time on the pb(II) and Cd(II) ion adsorption. Figure (7) showed an increase in the elimination removing percentages of the metal ions by increasing the period of contacting till reaching the equilibrium. The adsorption amount was high in the beginning because there is a large adsorption surface area suitable for attaching the pb(II) and Cd(II) ions. At the end the adsorption rate is slower probably due to that the active sites become saturated and equilibrium is stabilized (El-Ashtoukhy *et al.*, 2008; Pehlivan *et al.*, 2009). The contact time has been reached at 60min for pb(II) and 90min for Cd(II). As for the percentage of items removed in the $NiFe_2O_4$ nanoparticles for pb(II) and Cd(II) were found to be 61.74% and 64.30%, respectively.
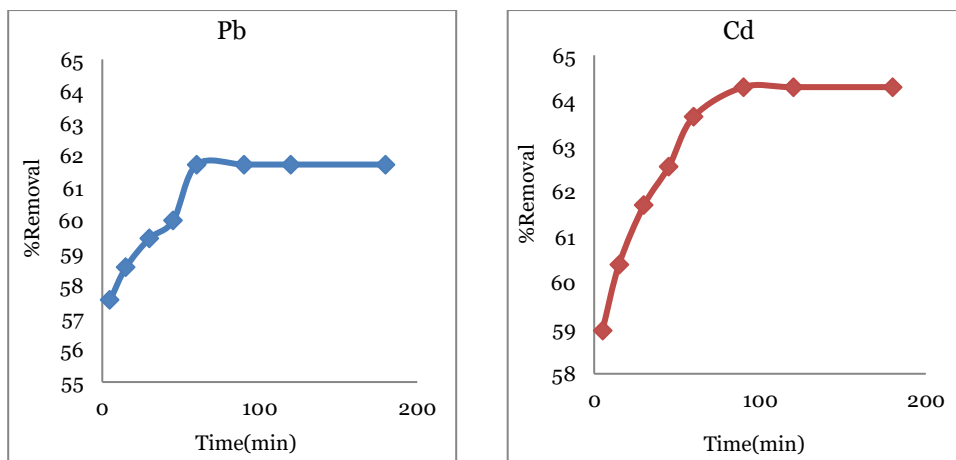

Figure 7. Effect of contact time on adsorption of pb(II) and Cd(II) ions onto $NiFe_2O_4$.

Effect of pH on the Adsorption:

Acidity is a significant aspect that affects the adsorption of heavy metals in aqueous solutions during solid-water interfaces. The accessibility in the solution of metal ions and the Link sites of the adsorbent are affected by pH (Adamson and Gast, 2001). The influence of pH on the adsorption of pb(II) and Cd(II) ion on $NiFe_2O_4$ nanoparticles in various pH (3, 5, 7 and 9) were studied by using affixed concentration and time contact of 60, 90min for pb(II) and Cd(II), respectively at 25°C (Fig.8). It showed the effect of pH on the adsorption process.

The present results indicated an increase in the removal of Pb(II) and Cd(II) percentage toward the base. The active sites gain a positive charge in the presence of an acidic medium (low pH) with the presence of hydronium ions, leading: to the repulsion between the positive charge metals and the adsorbent. Binding sites begin to deprotonate at higher pH values, making various functional groups accessible for binding the metal.

In general, As the pH increase, cation binding increases; however, as pH rises, the solubility of Pb(II) and Cd(II) ions decreases, resulting in an increase in the adsorption affinity towards the surfaces of $NiFe_2O_4$ (Esposito *et al.*, 2002; Lund, 1994). Accordingly, the pH values of 5 and 7 for pb(II) and Cd(II), respectively were chosen to carry out the experiment to avoid uncertain results, as other mechanisms such as sedimentation plays a turn in removing the metals.
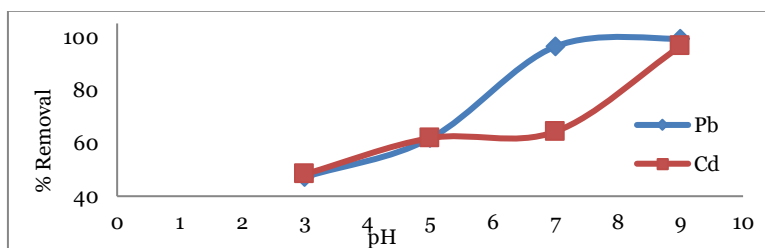

Figure 8. Effect of pH on Pb(II) and Cd(II) adsorption on $NiFe_2O_4$.

Adsorption Isotherm:

Various temperatures (10, 25, 37.5 and 50°C), were selected to assess the capacity of nanoparticles $NiFe_2O_4$ to remove ions Pb(II) and Cd(II) from their aqueous solutions. Figure (9) showed the isothermal adsorption of Pb(II) and Cd(II) ions and the amount of adsorbent on $NiFe_2O_4$ planned at occupying the balance concentricity (C_e).
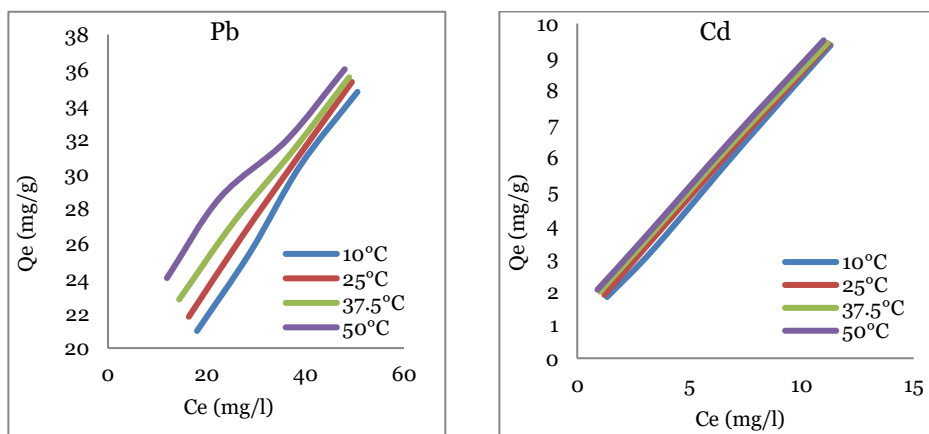

Figure 9. Adsorption isotherm of Pb(II) and Cd (II) on $NiFe_2O_4$ at different temperatures.

The isothermal adsorbent of Pb(II) and Cd(II) ions form on nanoparticles $NiFe_2O_4$ conforms to the Giles classification of the (S-type). The S-curve reveals the vertical or flat alignment of the adsorption, there is a strong attraction between the molecules within the adsorbent layer as the molten layer is actually adsorbed, where additional quantities are fixed (Giles *et al.*, 1960). The adsorption results were applied in practice using the Freundlich and Langmuir isotherm. The effects were followed up by using Freundlich's (eq. 7) and Langmuir's (eq. 8) (Veena and Robert, 2002), and Table (3) shows the data of isotherm adsorption.

Log Qe = log Kf + 1/n log Ce...............(7)

Where Kf is a function of adsorption capacity and n is the adsorption intensity.

Ce/Qe = 1/Qmb + Ce/Qm ....(8)

Where Q_m is the maximum adsorption capacities (mg/g) and b is related to the sorption energy.

The Freundlich and Langmuir isotherms are applied to the absorbance experimental data of Pb(II) and Cd (II) ions on $NiFe_2O_4$ nanoparticles from drawing log Qe opposite log Ce and Ce/Qe opposite Ce, respectively (Figs. 10 and 11). The results in Table (1) the R^2 values for the Freundlich model are closer to unity than Langmuir for adsorption process onto $NiFe_2O_4$, this proves that the application of the Freundlich model was better in characterizing the Pb(II) and Cd(II) ions adsorption on $NiFe_2O_4$ nanoparticles than the Langmuir models and it is the most accurate characterization of the multi-layer adsorption method on the surface of a heterogeneous adsorbent surface (Barrow, 1988).

Table 3. Results of the application of Freundlich and Langmuir isotherms on the system studied.

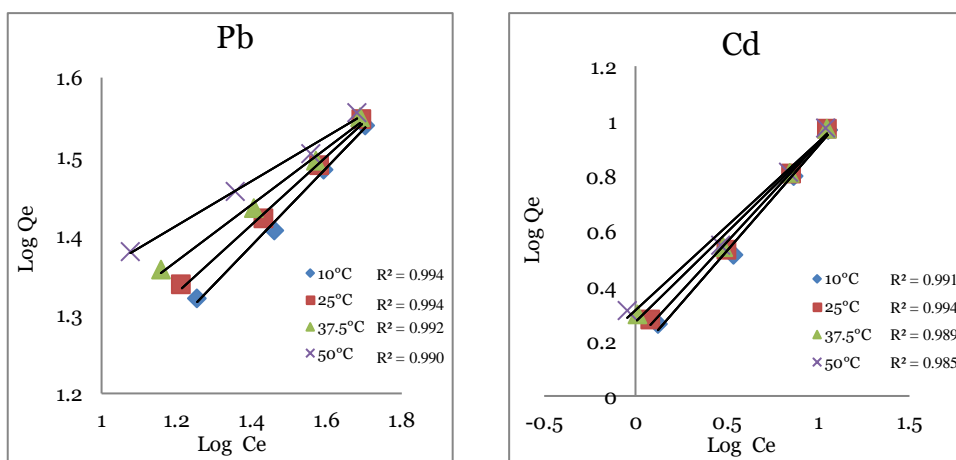| Ion	Temp. (C)	Langmuir Constants			Freundlich Constants		
		Q_m (mg/g)	b (l/mg)	R^2	n	Kf	R^2
Pb(II)	10.0	55.285	0.032	0.977	2.027	4.974	0.994
	25.0	51.085	0.042	0.982	2.310	6.422	0.994
	37.5	46.531	0.061	0.986	2.791	8.661	0.992
	50.0	42.533	0.099	0.989	3.544	11.855	0.990
Cd(II)	10.0	23.474	0.054	0.758	1.309	1.397	0.991
	25.0	19.531	0.075	0.863	1.388	1.583	0.994
	37.5	16.366	0.107	0.856	1.538	1.860	0.989
	50.0	15.220	0.130	0.845	1.635	2.050	0.985

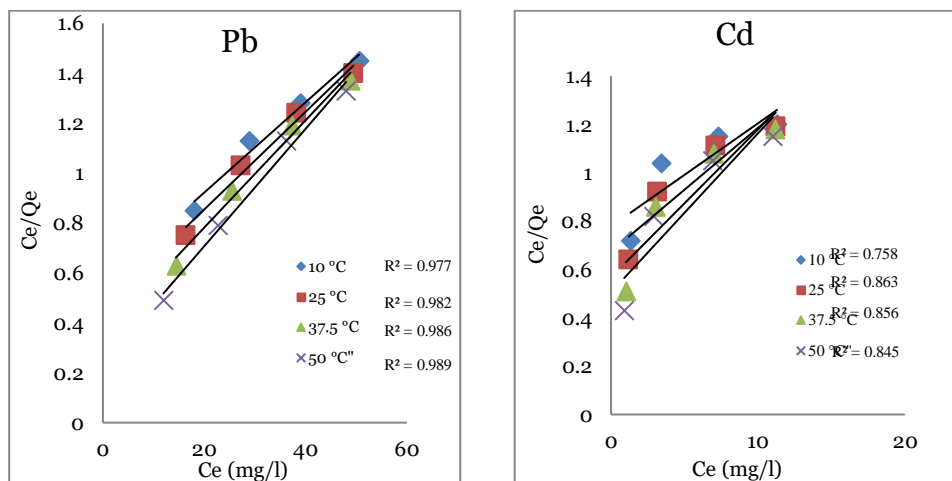Figure 10. Linear form of Freundlich isotherms of Pb(II) and Cd(II) on $NiFe_2O_4$ at different temperatures.

Figure 11. Linear form of Langmuir isotherms of Pb(II) and Cd(II) on NiFe₂O₄ at different temperatures.

The study of thermodynamics:

The effect of temperature on Pb(II) and Cd(II) ions adsorption was investigated using various initial concentrations and temperatures ranging from (10-50°C). The parameters of thermodynamic are represented by (ΔG), (ΔH), and (ΔS) was used to assess the feasibility the adsorption method, as shown in Table (4).

The relationship was linear between lnK against. $1/T$ with the correlation coefficient ($R^2 = 0.954 - 0.993$) and ($0.923 - 0.998$) for Pb(II) and Cd(II) ions, respectively adsorption on of NiFe₂O₄ nanoparticles (Fig. 12).

As seen from Table (3) represented, the enthalpy values (ΔH) of adsorption of ions Pb(II) and Cd(II) on nanoparticles NiFe₂O₄. The results indicated a positive value, which means that the adsorbent process is endothermic (Kapoor, 1994). The positive value of ΔS during the adsorption process is expressed that there is an increase in the randomness as a result of the interference between liquid and solid (Al-Saadie and Jassim, 2010), while the value of ΔG is negative and all temperatures had values increased with increasing temperatures, which indicates that the adsorption process occurs spontaneously (Hefne *et al.*, 2008).

Table 4. Thermodynamic functions for adsorption of Pb(II) and Cd(II) ions.

| Ion	Co (mg/l)	K				-ΔG				ΔH	ΔS
		Temperature									
		283	298	310.5	323	283	298	310.5	323		
Pb(II)	60	2.327	2.660	3.160	4.020	1.664	2.294	2.819	3.344	10.222	0.042
	80	1.767	1.943	2.136	2.522	1.082	1.487	1.824	2.162	6.559	0.027
	100	1.563	1.613	1.673	1.766	0.844	1.009	1.146	1.284	2.269	0.011
	120	1.372	1.427	1.454	1.501	0.606	0.726	0.826	0.926	1.658	0.008
Cd(II)	5	2.759	3.132	3.901	4.555	2.119	2.749	3.274	3.799	9.767	0.042
	10	1.915	2.154	2.311	2.424	1.440	1.755	2.017	2.280	4.503	0.021
	20	1.732	1.801	1.853	1.898	1.101	1.251	1.376	1.501	1.729	0.010
	30	1.654	1.676	1.688	1.729	1.196	1.301	1.388	1.476	0.785	0.007
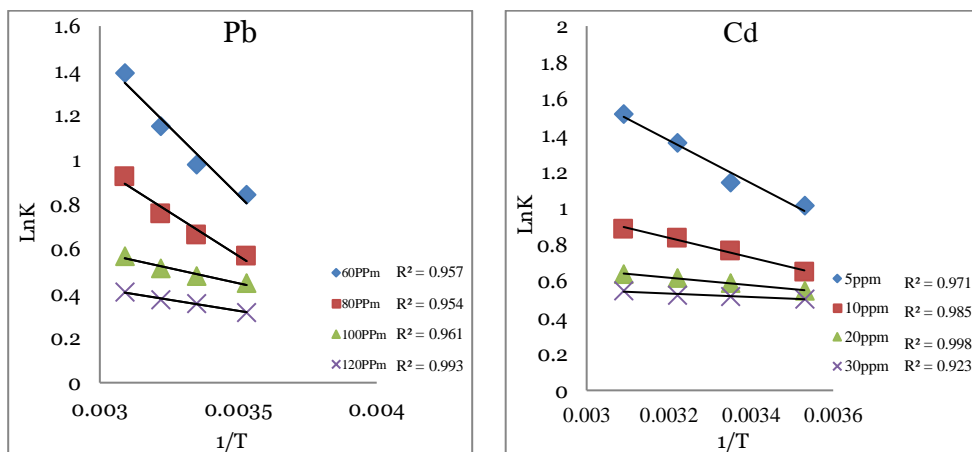
Figure 12.   Plot of lnK against 1/T for adsorption of Pb(II) and Cd(II) ions on $NiFe_2O_4$ nanoparticles.

Conclusion

In the present study, $NiFe_2O_4$ nanoparticles ferrites were prepared by sol-gel auto-combustion process and lemon juice, which is surfactant and a fuel agent. A single-stage spinel ferrite was obtained by sample calcining the sample at 600°C. The BET surface area analyses showed that the composite materials have a large surface area. The effect of different variables on the adsorption capacity, such as contact time, initial concentration of ions, the effect of pH and temperature, were studied. The contact time was at 60min for lead ion, 90min for cadmium ion. The effect of pH with range of 3-9 was studied. The study showed that the percentage of removal of lead ion is 61.47% and cadmium ions 64.30%. The isothermal adsorption was calculated using the models of Langmuir and Freundlich, as it was observed that the Freundlich model was more suitable for adsorption compared to the Langmuir model. As the adsorption reaction was automatic and endothermic according to thermodynamic properties, the prepared compound can be used as a heavy metal adsorbent and considered an important application to preserve the environment.

References

Abdel-Latif, I.A. 2012. Fabrication of Nano-Size Nickel Ferrites for Gas Sensors Applications. J. Phys., 1(2): 50-53.

Adamson, A.W. and Gast, A.P. 2001. Physical Chemistry of Surfaces, 6th ed., John Wiley and Sons, Inc., New York.

Al-Saadie, K.A. and Jassim, S.B. 2010. Adsorption study for chromium on Iraqi Bentonite. J. Bagh. Sci., 7(1): 745-756.

Anandan, K. and Rajendran,V. 2011. Morphological and size effects of NiO nanoparticles via solvothermal process and their optical properties. Mater. Sci. Semicond. Process, 14(1): 43-47.

Baig, N., Nadagouda, M. and Varma, R.S. 2015. Magnetically retrievable catalysts for asymmetric synthesis. Coord. Chem. Rev., 287: 137-156.

Baig, R.B.N. and Varma, R.S. 2013. Magnetically retrievable catalysts for organic synthesis. Chem. Commun., 49: 752-770.

Barrow, G.M. 1988. Physical chemistry. 5th ed., McGraw-Hill, New York, pp: 310-344.

Chai, L., Wang, Y., Zhao, N., Yang, W. and You, X. 2013. Sulfate-doped Fe_3O_4/Al_2O_3 nanoparticles as a novel adsorbent for fluoride removal from drinking water. J. Water Res., 47: 4040-4049.

Chen, S., Zou, Y., Yan, Z., Shen, W., Shi, S., Zhang, X. and Wang, H. 2009. Carboxy methylated bacterial cellulose for copper and lead ion removal. J. Haz. Mat., 161: 1355-1359.

Chen, Y., Ye, W., Yang, X. and Deng, F. 2011. Effect of contact time, pH and ionic strength on Cd (II) adsorption from aqueous solution onto bentonite from Gaomiaozi. China. J. Environ. Earth Sci., 64: 329-336.

Cullity, B.D. 1978. Elements of X-ray Diffraction. Addison-Wesley, London, 2nd ed.

Dehghanpour, H.R. 2016. Physical and Chemical Properties of $NiFe_2O_4$ Nanoparticles Prepared by Combustion and Ultrasonic Bath Methods. Russian J. Appl. Chem., 89(1): 80-83.

El-Ashtoukhy, E., Amina N.K. and Abdelwahab, O. 2008. Removal of lead (II) and copper (II) from aqueous solution using pomegranate peel as a new adsorbent. Journal of Desalination, 223: 162-173.

Esposito, A., Pagnanelli, F. and Veglio, F. 2002. pH-related equilibria models for biosorption in single metal systems. J. Chem. Engin. Sci., 57: 307-313.

Ge, H. and Ma, Z. 2015. Microwave preparation of triethylenetetramine modifed graphene oxide/chitosan composite for adsorption of Cr(VI). J. Carbo. Poly. 131: 280-287.

Gholipour, N. and Rahimi-Nasrabadi, M. 2019. Auto-combustion preparation and characterization of $BaFe_2O_4$ nanostructures by using lemon juice as fuel. J. Chem. Methodol., 3: 276-282.

Giles, C.H., MamEwans, T.H., Nakhwa, S.N. and Smith, D. 1960. Studies in adsorption. A system of classification of solution adsorption isotherms, and its use in diagnosis of adsorption mechanisms and in measurement of specific surface areas of solids. J. Chem. Soc., 786: 3973-3993.

Hefne, J.A., Mekhemer, W.K., Alandis, N.M., Aldayel, O.A. and Alajyan, T. 2008. Kinetic and thermodynamic study of the adsorption of Pb(II) from aqueous solution to the natural and treated bentonite. International Journal of Physical Sciences, 3(11): 281-288.

Ismat, B., Nosheen, N., Munawar, I., Shagufta, K., Haq, N., Shazia, N., Yursa, S., Kashif, J., Misbah, S., Sadia, A., Fariha, R. and Mazhar, A. 2017. Green and eco-friendly synthesis of cobalt-oxide nanoparticle: Characterization and photo-catalytic activity. J. Adv. Powder Technol., 28: 2035-2043.

Ivanov, V., Tay, J.H., Tay, S.T.L. and Jiang, H.L. 2004. Removal of micro-particles by microbial granules used for aerobic wastewater treatment. J. Water Sci. Technol., 50: 147-154.

Jain, P., Kaur, M., Kaur, M. and Grewal, J.K. 2019. Comparative studies on spinal ferrite MFe_2O_4 (M=Mg/Co) nanoparticles as potential adsorbents for Pb(II) ions. Bull. Mater. Sci., 77: 1-9.

Kapoor, K.L. 1994. A Text Book of Physical Chemistry. Macmillam India Limited, India, pp: 449-481.

Kareem, Sh.J. and Rajeh, A.A.H. 2018. The effect of catalyst type on the microstructure and magnetic properties of synthesized hard cobalt ferrite. Nanoparticles, 26(4): 282-291.

Kavas, H., Kasapoglu, N., Baykal, A. and Kaseoglu, Y. 2009. Characterization of $NiFe_2O_4$ nanoparticles synthesized by various methods. Chem. Papers., 63(4): 450-455.

Kefeni, K.K., Mamba, B.B. and Msagati, T.A.M. 2017. Application of spinel ferrite nanoparticles in water and wastewater treatment: A Review. Sep. Purif. Technol., 188: 399-422.

Khoshkerdar, I. and Esmaeili, H. 2019. Adsorption of Cr(III) and Cd(II) ions using Mesoporous Cobalt-Ferrite Nanocomposite from Synthetic Wastewater. Acta. Chem. Slov., 66: 208-216.

Liu, F., Zhou, K., Chen, Q., Wang, A. and Chen, W. 2018. Comparative study on the synthesis of magnetic ferrite adsorbent for the removal of Cd(II) from wastewater. Adsorption Sci. and Tech., 36: 1456-1469.

Lund, W. 1994. The Pharmaceutical Codex. 12th ed., The Pharmaceutical Press, London, pp: 774-8512.

Luo, X., Zeng, J., Liu, S. and Zhang, L. 2015. An effective and recyclable adsorbent for the removal of heavy metal ions from aqueous system: Magnetic chitosan/cellulose microspheres. Bioresour. Technol., 194: 403-406.

Maaz, K., Karim, S., Mumtaz, A., Hasanain, S.K., Liu, J. and Duan, J.L. 2009. Synthesis and magnetic characterization of nickel ferrite nanoparticles prepared by coprecipitation route. J. Magn. Magn. Mater., 321(12): 1838-1842.

Masunga, N., Mmelesi, O.K., Kefeni, K.K. and Mamba, B.B. 2019. Recent advances in copper ferrite nanoparticles and nanocomposites synthesis, magnetic properties and application in water treatment. J. Environ. Chem. Eng., 7: 103-179.

Nejati, K. and Zabihi, R. 2012. Preparation and magnetic properties of nano size nickel ferrite particles using hydrothermal method. Chem. Cent. J., 6(1): 23-28.

Pehlivan, E., Altun, T. and Parlayıcı, S. 2009. Utilization of barley straws as biosorbents for $Cu2^+$ and $Pb2^+$ ions. J. Hazard. Mater., 164: 982-986.

Prasad, S. and Gajbhiye, N.S. 1998.Magnetic studies of nanosized nickel ferrite particles synthesized by the citrate precursor technique. J. Alloys Compd., 265(1-2): 87-92.

Salavati-Niasari, M., Davar, F. and Mahmoudi, T. 2009. A simple route to synthesize nanocrystalline nickel ferrite ($NiFe_2O_4$) in the presence of octanoic acid as a surfactant. Polyhedron, 28(8): 1455-1458.

Seiler, H.G., Sigel, H. and Sigel, A. 1988. Handbook on toxicity of inorganic compounds. New York, Marcel Dekker, pp: 251-264.

Sezgin, N., Sahin, M.S., Yalcin, A. and Koseoglu, Y. 2013. Synthesis, characterization and the heavy metal removal efficiency of MFe_2O_4 (M=Ni, Cu) Nanoparticles. Ekoloji, 22(89): 89-96.

Shi, Y., Ding, J., Liu, X. and Wang, J. 1999. $NiFe_2O_4$ ultrafine particles prepared by coprecipitation/mechanical alloying. J. Magn. Mater., 205(2-3): 249-254.

Tan, X., Li, G., Zhao, Y. and Hu, C. 2009. Effect of Cu content on the structure of $Ni1-xCuxFe_2O_4$ spinels. Mater. Res. Bull., 44(12): 2160-2168.

Tran, Ch.V., Quang, D.V., Thi, H.Ph.N., Truong, T.N. and La, D.D. 2020. Effective removal of Pb(II) from aqueous media by a new design of Cu-Mg binary ferrite. ACS. Omega, 5: 7298-7306.

Veena, M. and Robert, H.H. 2002. The role of F-400 granular activated carbon in scavenging dissolved copper ions from aqueous solution. Journal of Energeia, 13: 1-4.

Wang, J. and Chen, C. 2009.Biosorbents for heavy metals removal and their future. Biotechnol. Adv., 27: 195-226.

Wang, J., Zeng, C., Peng, Z. and Chen, Q. 2004. Synthesis and magnetic properties of Zn1-xMnxFe2O4 nanoparticles. Physica B. Cond. Matt., 349(1-4): 124-128.

Yadanaparthi, S.K.R., Graybill, D. and Wandruszka, R.V. 2009. Adsorbents for the removal of arsenic, cadmium, and lead from contaminated waters. J. Hazard. Mater., 171: 1-15.

Yavuz, C.T., Mayo, J.T., Yu, W.W., Prakash, A., Falkner, J.C., Yean, S., Cong, L., Shipley, H.J., Kan, A., Tomson, M., Natelson, D. and Colvin, V.L. 2006. Low-field magnetic separation of monodisperse Fe3O4 nanocrystals. J. Sci., 314: 964-967.

Yin, P., Xu, Q., Qu, R., Zhao, G. and Sun, Y. 2010. Adsorption of transition metal ions from aqueous solutions onto a novel silica gel matrix inorganic–organic composite material. J. Hazard. Mater., 173: 710-716.

استخدام المواد المغناطيسية النانوية لإزالة أيونات الكادميوم (II) والرصاص (II) من المحاليل المائية

احمد يوسف حمود[1], طارق زباري جاسم[2] ومهند جواد الأسدي[2]

[1] مركز علم البحار، [2] كلية التربة للعلوم الصرفة، جامعة البصرة — العراق

المستخلص ـ حضرت جسيمات الفرايتات النانوية (NPs) ذات الصيغة $NiFe_2O_4$ بطريقة السول ـ جل ذات الاحتراق التلقائي باستخدام عصير الليمون كعامل خافض للشد السطحي ووقود للتفاعل. وتقع هذه الطريقة ضمن الكيمياء الخضراء وهي طريقة صديقة للبيئة وباقل كلفة من الطرق الاخرى. شخصت المواد النانوية باستخدام تقنيات فيزيائية وكيميائية مختلفة: جهاز تحليل المساحة السطحية -Brunauer- Emmett-Teller (BET)، تقنية المجهر الالكتروني الماسح ذات مجال الانبعاث الضوئي (FE-SEM)، أطياف الأشعة السينية المشتتة للطاقة (EDX)، مطيافية الأشعة تحت الحمراء (FTIR)، المجهر الإلكتروني النافذ (TEM) وحيود الأشعة السينية (XRD). تناول البحث احد تطبيقات ظاهرة الامتزاز من المحاليل المائية، إذ درس امتزاز ايونات الرصاص والكادميوم على سطح المادة النانوية المحضرة, لغرض الحصول على سطح يمتلك قابلية عالية على امتزاز ايونات الرصاص والكادميوم بهدف معالجة المياه الملوثة بآيونات هذه العناصر. درس تأثير المتغيرات المختلفة على سعة الامتزاز مثل زمن الاتزان والتركيز الابتدائي للايونات والدالة الحامضية ودرجة الحرارة, كان زمن الاتزان عند (60) دقيقة لايون الرصاص, (90) دقيقة لايون الكادميوم. كما درس تأثير الدالة الحامضية وبالمدى (9-3). اظهرت الدراسة ان النسبة المئوية للازالة لايون الرصاص 61.47% ولايون الكادميوم 64.30%. استخدمت النتائج التي تم الحصول عليها من دراسة تأثير درجة الحرارة في تطبيق المعادلات الرياضية لايزوثيرمات لانكماير وفريندلش على البيانات العملية للامتزاز, فقد أعطى ايزوثيرم فريندلش علاقة خطية بمعاملات ارتباط جيدة أفضل من ايزوثيرم لانكماير. بينت الدراسة الثرموديناميكية ان عملية الامتزاز ماصة للحرارة من قيم لـΔH الموجبة, وتلقائية من القيم السالبة لـ ΔG, بينما دلت القيم الموجبة لـ ΔS على زيادة العشوائية لعملية الامتزاز.